

MOMENT-CURVATURE ANALYSIS OF COUPLED BENDING AND MECHANOSORPTIVE RESPONSE OF RED SPRUCE BEAMS

*Rastislav Lagaňa**

Research Scientist
Technical University in Zvolen
96053 Zvolen, Slovakia

William G. Davids

Professor
The Advanced Structures and Composites Center
University of Maine
Orono, ME 04469-5793

Lech Muszyński†

Assistant Professor
Department of Wood Science and Engineering
Oregon State University
Corvallis, OR 97331-5751

Stephen M. Shaler†

Professor and Associate Director
The Advanced Structures and Composites Center
University of Maine
Orono, ME 04469-5793

(Received December 2010)

Abstract. In this study, an expanded comprehensive numerical approach to predict hygromechanical behavior of beams is proposed that rigorously couples spatially varying time-dependent moisture content fluctuation with uniaxial stress–strain relations. The constitutive model, consisting of elastic, viscoelastic, and two mechanosorptive strain elements connected in series, was used in a layered moment-curvature flexural analysis. The procedure is numerical and is able to take into account effect of moisture content changes, different mechanosorptive behavior in tension and compression, and cross-sectional hygroexpansion. The overall trend and magnitude of predicted deflections are in good agreement with experimental results. Results demonstrated that complex beam behavior in a varying environment can be predicted by a simple model with well-defined material characteristics generated through relatively simple 18-h uniaxial experiments.

Keywords: Bending, creep, mechanosorption, modeling, spruce, compression, tension.

INTRODUCTION

Mechanosorptive (MS) behavior of wood is defined as additional deformation developed during simultaneous loading and moisture content (MC) changes (Hunt 1994). It is triggered by changes in MC below FSP and cannot be ex-

plained by simple superposition of viscoelastic (VE) (immediate and delayed) and hygro-expansive deformations. MS effect was first indirectly reported in the early 1950s in studies on swelling pressure of wood (Perkitny 1951). Since then, it has been the subject of extensive research by many investigators. The current state of knowledge was summarized by Wang (1991), Hunt (1994), Ranta-Maunus (1994), Hanhijärvi (2000), and most recently Muszyński et al

* Corresponding author: lagana@vsld.tuzvo.sk

† SWST member

(2005). Since the 1970s, this phenomenon has been generally treated as separate from VE creep (Grossman 1976) and may be of the same magnitude or greater than VE creep for in-service wood beams (Mårtensson 1994).

Many models have been developed to describe the hygromechanical behavior of wood. Most of them may be roughly divided into two major categories or types: Maxwell type and Kelvin type (Hanhijävi 2000). Maxwell-type models describe MS behavior using a constitutive equation similar to that of Newtonian fluid, in which the time variable is replaced by a monotonic measure of cumulative MC changes (Rybarczyk 1973; Plevris and Triantafillou 1995; Lu and Leicester 1997; Davids et al 2000). These models, however, cannot describe recovery of MS creep when load is removed while MC changes continue. Kelvin-type models use the constitutive equation of Kelvin body in a similar manner, which may be illustrated as a parallel arrangement of the Newton-like MS term just described and a spring (Rybarczyk 1973; Salin 1992; Omarsson et al 1998; Omarsson 1999). Kelvin-type models can describe decreasing MS creep rates. These effects, however, have been shown to be insignificant in short-term experiments (Muszyński and Olejniczak 1996).

It is also generally assumed that MS creep occurs in a similar manner during both wetting and drying (Hanhijävi 1995). Some researchers have made efforts to build models that include MS and VS terms in one constitutive equation (Leicester 1971; Bazant 1985; Yahiaoui 1991; Hanhijävi 1995), which sometimes leads to convoluted formulas operating simultaneously in two variable domains: time and cumulative MC.

Coupling of VE and MS deformations requires that proposed material models assume a mutual effect of these components on each other. A small, although presumably significant, effect of MS creep on VE creep rate has been reported by Hanhijävi and Hunt (1998). In contrast, Navi et al (2002) observed that duration of load and VE creep rate have a small effect on MS creep, and therefore, VE and MS creep could be

treated as independent features. This contradiction appears to arise from lack of agreement on what actually constitutes MS effect and how it should be defined.

The simple conceptual distinction proposed in this article is based on the combination of three different trigger mechanisms for each strain component (load, time, and change of MC below FSP), although in reality MS deformation, as a second-order phenomenon, is always accompanied by VE deformations and free swelling or shrinkage. Consequently, MS deformation cannot be measured directly or easily isolated. However, once MS effect is defined as the additional deformation that cannot be expressed as simple superposition of VE and free hygroexpansion, further assumptions about effect of duration of load on MS deformation or effect of stress on free hygroexpansion appear to be conceptual errors resulting from secondary “redistribution” of the MS component.

The difficulty in modeling flexural behavior of wood subjected to sustained loads and varying climates lays in the fact that in beams, the nonuniform stress pattern across the cross-section is coincident with nonuniform MC changes resulting from external climate changes (Muszyński et al 2005). This poses fundamental difficulties when it comes to separation of strain components and interpretation of test results (Ranta-Maunus and Gowda 1994). For example, even in the absence of creep and MS, concurrent effects of local MC changes on the cross-section dimensions (constrained shrinkage/swelling of the section) and on elastic modulus produce counteracting effects on flexural stiffness.

In addition, different MS behavior in tension and compression has been observed in several experimental studies (Bengtsson 1999; Toratti and Svensson 2000; Lagaña et al 2004; Muszyński et al 2006; Strömbro and Gudmundson 2008). The authors are unaware of any models that incorporate different MS response of wood in compression and tension. It has been noted in this literature that the difference between tensile and compressive MS is expressed as “slightly

different” perpendicular to grain (Toratti and Svensson 2000) or “larger in compression” in the axial direction (Bengtsson 1999). As suggested by Strömbro and Gudmundson (2008), significant differences in tension and compression MS creep behavior in the article are probably an effect of geometrical fiber properties (fibers curl and kink). In solid wood, this local buckling may occur in amorphous regions of wood cellulose compressed in an axial direction during MC changes.

Because local MC strongly affects mechanical characteristics of wood, when modeling structural behavior of beams, the stress–strain analysis must be coupled with a rigorous diffusion analysis as has been done in several studies (Toratti 1992; Hanhijärvi 1995; Omarsson 1999). The approach of using average MC across the cross-sections of beams is not sufficient when analyzing complex hygromechanical behavior (Muszyński et al 2005). Another trend in the field is that some models are validated against experiments that use the same specimen sizes, load, and climate conditions that were used to derive the models. This approach often results in fairly convoluted models being proposed to explain poorly designed experiments and then being successfully validated against the same empirical data, although they could be used for limited testing or service conditions.

The first objective of this study was to improve the existing constitutive model framework that accounts for different MS and VS responses of wood in tension and compression. This approach was used to predict long-term behavior of wood beams exposed to varying climate conditions using MS properties derived from 18-h tensile and compression tests conducted in a separate study (Muszyński et al 2005). The second objective was to demonstrate that complex beam behavior in varying environments can be predicted by means of a simple model and well-defined material characteristics generated by relatively simple uniaxial experiments. Results of simulations using this model were compared with measured bending responses of beams subjected to cyclic climate change.

MODEL DESCRIPTION

Overview

This study builds on previous research in which MS properties were determined from material level tests. The overall approach involved measuring mechanical properties (while minimizing effects of MC and stress distribution) and diffusion properties of red spruce on the material level (Lagaña 2005). In this study, these properties were model inputs for simulating behavior of samples of different geometry and subjected to different loading and climate conditions. Subsequently, results of simulations were compared with measured behavior of real beams in varying conditions.

As explained, local MC changes in beam sections affect local VE (immediate and delayed) compliances of wood and trigger a local MS response, whereas overall change in MC makes the cross-section shrink or swell (Muszyński et al 2005). Because of that complex effect, local stiffness across the beam cross-section changes with local MC as well as internal stress distribution across the depth of the beam (Ranta-Maunus and Gowda 1994).

An approach used in this study was to couple moisture transport over the beam cross-section with flexural analysis (Davids et al 2000; Moutee and Fortin 2007) and a constitutive model that accounted for different MS compliance characteristics under tension and compression. Model parameters must be functions of time, MC, and MC change. MC variation with time and space were computed using a two-dimensional finite difference scheme and assumed to be identical along beam length, which is reasonable given the relative insignificance of end effects on deflection.

Constitutive Model

The uniaxial constitutive model (Fig 1) consists of four elements connected in series (similar to Toratti 1992). The governing equations are

$$\sigma = E\varepsilon_e \quad (1)$$

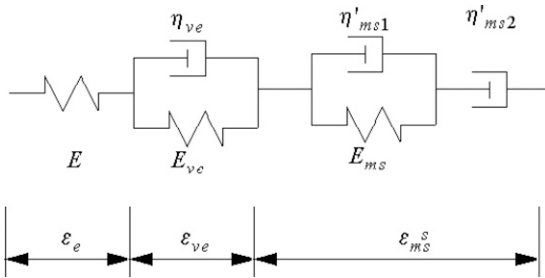


Figure 1. Uniaxial constitutive model.

$$\sigma = E_{ve}\epsilon_{ve} + \eta_{ve} \frac{\partial \epsilon_{ve}}{\partial t} \tag{2}$$

$$\sigma = E_{ms}\epsilon_{ms1} + \eta'_{ms1} \frac{\partial \epsilon_{ms1}}{\partial t} \tag{3}$$

$$\sigma = \eta'_{ms2} \frac{\partial \epsilon_{ms2}}{\partial t} \tag{4}$$

$$\epsilon = \epsilon_e + \epsilon_{ve} + \epsilon_{ms1} + \epsilon_{ms2} \tag{5}$$

In Eqs 1-4, σ represents stress. The strain components are elastic strain ϵ_e , delayed (VE) strain ϵ_{ve} , and MS strain, which is the sum of ϵ_{ms1} and ϵ_{ms2} (tension or compression). The modulus of elasticity E is a MC-dependent property. The parameters E_{ve} and η_{ve} make up the Kelvin term, whereas E_{ms} , η'_{ms1} , and η'_{ms2} are parameters of two MS terms: the Kelvin-type (as first proposed by Rybarczyk [1973] and Salin [1992]) and the Newton-type arranged in series. Both η'_{ms1} and η'_{ms2} are inversely related to the absolute value of the time rate of change in MC, $|\frac{\partial u}{\partial t}|$ as follows:

$$\eta'_{ms1} = \frac{\eta_{ms1}}{|\frac{\partial u}{\partial t}|} \text{ and } \eta'_{ms2} = \frac{\eta_{ms2}}{|\frac{\partial u}{\partial t}|} \tag{6}$$

where η_{ms1} and η_{ms2} are MS constants that differ for compression and tension, respectively. In this study, MS creep parameters for compression and tension were initially assumed equal and then the compression parameter was gradually adjusted within the range reported in other studies until good matching with experimental results was obtained. This was the only parameter adjusted ex-post because of the scarcity of reliable MS data for compression along the grain.

Hygroexpansion in the longitudinal direction was not considered in the analysis, because it had a very small effect on flexural deformation of a simply supported beam during symmetrical MC changes across the cross-section.

Using Eqs 1 and 5, Eqs 2, 3, and 4 can be rearranged into a system of ordinary differential equations (ODEs):

$$\frac{d\epsilon_{ve}}{dt} = \frac{1}{\eta} [E(\epsilon - \epsilon_{ve} - \epsilon_{ms1} - \epsilon_{ms2}) - E_{ve}\epsilon_{ve}] \tag{7}$$

$$\frac{d\epsilon_{ms1}}{dt} = \frac{1}{\eta'_{ms1}} [E(\epsilon - \epsilon_{ve} - \epsilon_{ms1} - \epsilon_{ms2}) - E_{ms}\epsilon_{ms1}] \tag{8}$$

$$\frac{d\epsilon_{ms2}}{dt} = \frac{1}{\eta'_{ms2}} [E(\epsilon - \epsilon_{ve} - \epsilon_{ms1} - \epsilon_{ms2})] \tag{9}$$

Eqs 7-9 were solved using a numerical time-stepping scheme. A numerical solution was required because of the explicit coupling of model parameters with the time-varying MC, which makes the system of ODEs nonlinear.

A variety of methods are available to solve systems of ODEs. In this study, the scientific and engineering computing package Matlab (Mathworks, Inc., Natick, MA) was used to implement the model. This allowed the use of a built-in ODE solver that relies on numerical differentiation formula functions, which are suitable for solving stiff problems such as those presented by Eqs 7-9.

Flexural Analysis

Time-dependent equilibrium requirements for the beam cross-section were enforced using a layered moment-curvature analysis. This approach has been used by several researchers (Lu and Leicester 1997; Muszyński 1997; Davids et al 2000). Internal axial force F_{in} and internal moment M_{in} are computed according to

$$F_{in} = \int_A \sigma dA \approx \sum_i^{n \times m} \sigma_i \Delta A_i = 0 \tag{10}$$

$$M_{in} = \int_A \sigma y' dA \approx \sum_i^{n \times m} \sigma_i y'_i \Delta A_i = M_{ex} \quad (11)$$

The beam cross-section was divided into an $n \times m$ element in the x and y directions, respectively. Stress is a function of strain and time, ΔA_i denotes area of an element i , and y'_i is its distance from the neutral axis. For four-point bending, external moment M_{ex} is easily computed using status at any point in the span. Area of an element as well as distance from the neutral axis varies with MC change because of transverse hygroexpansion. Because each element actually undergoes restrained shrinkage and swelling, three-dimensional modeling is required for evaluating beam cross-section area. To simplify the problem, average MC and tabulated values of transverse shrinkage and swelling coefficients (FPL 1999) were used across the entire cross-section. A similar approach was used by Hanhijärvi (1995).

Flexural strains were computed based on the assumption that plane sections remain plane after loading, so that total strain ϵ was linearly related to curvature ϕ :

$$\epsilon = \phi(y - \bar{y}) \quad (12)$$

where y is the distance of an element from the central axis and \bar{y} is the distance from the neutral axis to the central axis (Fig 2). Although any stress-strain relation can be used, a linear relation was used in this study, which represents the stress-strain response of wood at working stress levels.

At any time step k , the moment was evaluated for several chosen curvatures (ϕ) as follows. Because mechanical properties of wood differ in tension and compression zones despite symmetrical distribution of MC across the cross-section, the position of the neutral axis changes. Therefore, only one unknown \bar{y} from Eq 10 was numerically evaluated using the Newton-Raphson method. After that, the internal moment for a given curvature was computed from Eq 11. Moment curvature relation

$$\phi^k = f(M^k) \quad (13)$$

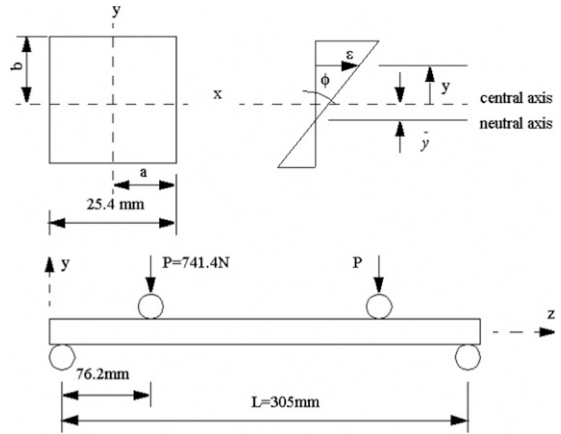


Figure 2. Geometry of cross-section, strain distribution across the beam, and loading of the simply supported beam.

was evaluated for each time step. The general beam equation, which can be simplified here for small deflections, is related to moment curvature relationship (Eq 13) as follows:

$$\frac{d^2 \Delta}{dz^2} \Big|_{\Delta \ll h} = \phi_z^k = f(M_z^k) \quad (14)$$

Deflection Δ at any point along the beam subjected to pure moment was calculated for each time step k . The coordinate z is parallel to beam length and h is beam depth. Eq 14 was solved numerically using a second-order accurate, centered finite-difference method. Boundary conditions for the simply supported beam were

$$\Delta|_0 = 0 \quad (15)$$

$$\frac{d\Delta}{dz} \Big|_{\frac{L}{2}} \quad (16)$$

Modeling Diffusion in Wood

At each time step, water concentration distribution across the beam section was calculated according to Fick's second law

$$\frac{\partial c}{\partial t} = \frac{\partial}{\partial x} \left(D_x \frac{\partial c}{\partial x} \right) + \frac{\partial}{\partial y} \left(D_y \frac{\partial c}{\partial y} \right) \quad (17)$$

and using the third-order boundary conditions (Crank 1979):

$$-D \frac{\partial c}{\partial x} \Big|_{x=a} = S [c_a - c_{eq}(T, RH)] \quad (18)$$

$$-D \frac{\partial c}{\partial y} \Big|_{y=b} = S [c_b - c_{eq}(T, RH)] \quad (19)$$

In Eqs 17-19, t , x , and y are time and space coordinates and D_x , D_y are coefficients of diffusion in the x and y directions. Surface emission factor S was taken from data published by Toratti (1992). The model geometry is 1/4 symmetric, therefore symbols a and b represent half the thickness in the x and y directions. The term c_{eq} represents equilibrium water concentration given by environmental conditions at temperature T and RH RH . D_x and D_y are water concentration-dependent. Stamm (1959) proposed the following relation based on Arrhenius exponential function of two parameters D_0 and B to quantify this dependence:

$$D = D_0 e^{-Bc} \quad (20)$$

Parameters D_0 and B were experimentally evaluated from distribution of MC during uniaxial drying in radial and tangential directions using the same material as for the bending test (Muszyński et al 2005). MC distribution across the cross-section was evaluated numerically using the second-order accurate Crank-Nicolson method (Gamache 2001). Distribution of MC across the beam was assumed to be symmetrical to the x and y axes.

MATERIALS AND METHODS

Material Preparation

Red spruce (*Picea rubens* Sarg.) logs were acquired from a tree in the Penobscot Experimental Forest in Maine. The tree was 100 yr old, and diameter at breast height was 380 mm. The trunk was sequentially cut into 400- to 500-mm logs in such a way that knot rings were removed. These logs were wrapped in plastic bags and stored in a freezer at -6°C to prevent

drying and decay. Each log was divided into 16 wedges ($25 \times 25 \times 350$ mm [$r \times t \times l$]). Eight of them were used to fabricate clear sapwood specimens for the bending test (Fig 3). Ends of all specimens were sealed with silicone to prevent diffusion from the transverse section. Two additional matched specimens were used to measure actual MC and free shrinkage and swelling of the cross-section. One specimen used to measure MC was placed on a scale balance (resolution 0.001 g). The other specimen was fixed in such way that free shrinkage and swelling could be measured in both radial and tangential directions (Fig 4).

Beam specimens were subjected to four-point bending in the tangential direction (Fig 2). Two load levels were used: four beams were loaded with 1482.8 N and four with 889.6 N, which created corresponding theoretical maximum flexural stress of approximately 50 and 30% of green bending strength, respectively. The experimental configuration, similar to the one used by Bengtsson (2001), is shown in Fig 5. Beam deflection was measured using linear conductive potentiometers with accuracy of 0.025 mm placed at midspan.

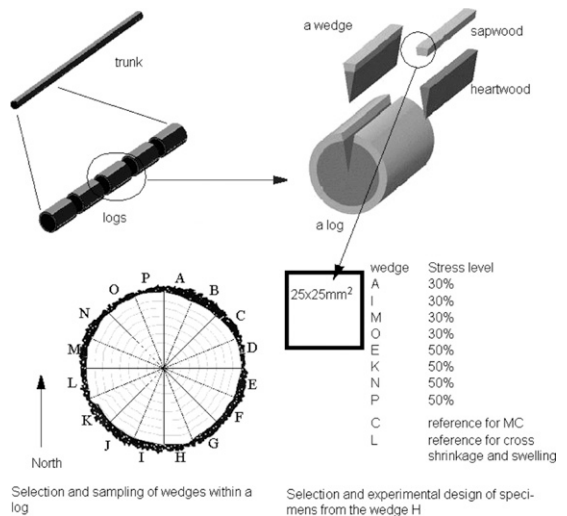


Figure 3. Selection of material used for measuring hygro-mechanical properties in bending.

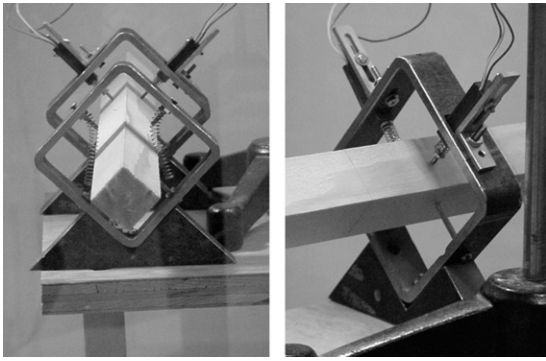


Figure 4. Placement of reference specimen for measuring shrinkage and swelling in radial and tangential directions.

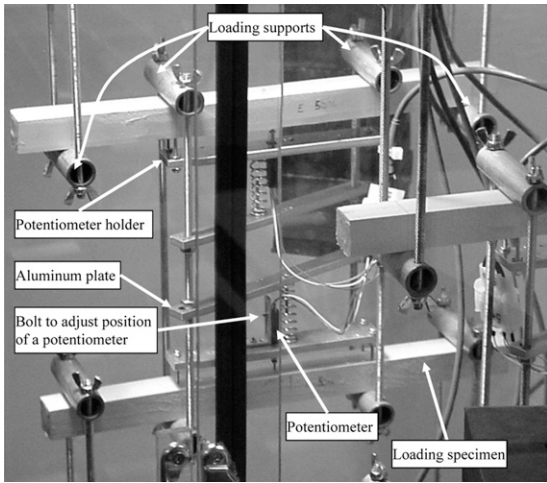


Figure 5. Loading of the beams. Front view detail.

Specimens (loaded and reference) were placed in a chamber with a controlled environment and were conditioned at 55% RH and constant temperature $T = 22^{\circ}\text{C}$ until a uniform equilibrium MC of 10% was reached. For the first 5 weeks after loading, RH was cyclically varied between 90 and 30% in 7-day cycles (Fig 6). After that, irregular humidity changes were allowed to test whether the model could also predict the effect of variable climate. The total experiment duration was 11 weeks.

Simulation

Initial MOE was evaluated from initial deflection of a tested specimen. Linear MC depen-

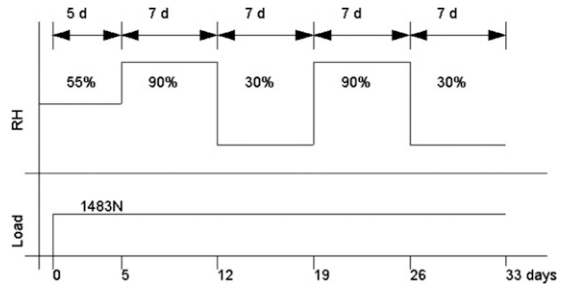


Figure 6. Environmental condition and loading schedule of bending specimens during the first 5 weeks of loading.

ency of MOE was evaluated by Muszyński et al (2006), and rate of change (b from Table 1) was assumed to be equal in tension and compression because of a lack of reliable compression data for red spruce. In reality, rate of change was higher in compression than in tension and is constant for specific ranges of MC (Kretschmann and Green 1996). Closer analysis of this feature is required if insight is to be gained on the immediate effect of MC. Fortunately, this feature, if more precisely defined, would result in an insignificantly different alteration of deflection caused by MC changes and would not affect overall deflection (see “Comments on Errors and Limitations”).

Creep at constant climate for 2-1/2 mo could not be reliably evaluated from parameters obtained from 18-h tests in tension and compression (Lagaña et al 2004; Muszyński et al 2006). Instead, VE creep parameter compliance was obtained from deflections measured during the first 5 da of loading at constant climate and was used to predict VE creep during subsequent MC fluctuations.

A three-parameter solid model was used to express VE compliance J_{ve} at constant climate:

$$J_{ve} = \frac{1}{E_0} + \frac{1}{E_0} \left(1 + e^{\frac{-E_1}{\eta} t} \right) \quad (21)$$

where E_0 , E_1 , and η are parameters of the creep model and t is duration of load. Linear VE behavior of wood was assumed so that compliance in bending J_{ve} could be directly related to measured deflection.

Table 1. Model parameters.

Material property	Notation	Value	Units	References
Hygroexpansion coefficients	k_{rad}	0.127	%/% of MC	FPL 1999
	k_{tan}	0.260		
Elastic modulus, $E = E_0 + bMC$	E_0	14.33	GPa	Muszyński et al 2006
	b	-11.84	GPa	
Creep at constant climate (MC = 9.9%)	E_1	119.1	GPa	This study
	η	4.497×10^{16}	Pa.s	
MS coefficients in tension	E_{MS}	38.09	GPa	Muszyński et al 2006
	η_{ms1}	1.984		
	η_{ms2}	219.5		
MS coefficients in compression	E_{MS}	37.18		Lagaña et al 2004
	η_{ms1}	2.094		
	η_{ms2}	6.906		
Diffusion coefficient, radial $D = D_0e^{-Bc}$	D_{0rad}	1.301×10^{-10}	$m^2.s^{-1}$	Lagaña 2005
	B_{rad}	0.01234	$m^3.kg^{-1}$	
Diffusion coefficient, tangential	D_{0tan}	1.161×10^{-10}	$m^2.s^{-1}$	
	B_{tan}	0.01134	$m^3.kg^{-1}$	
Surface emission factor, S	S	1.3×10^{-7}	$m.s^{-1}$	Toratri 1992

MC, moisture content; MS, mechanosorptive.

MS parameters in tension and compression were taken from experiments presented by Lagaña et al (2004) and Muszyński et al (2006). Parameters were taken across a range of cumulative MC up to 100%. A summary of parameters used for modeling is shown in Table 1.

Midspan deflection was calculated for a simply supported red spruce beam subjected to four-point bending (Fig 2). The beam cross-section was $25 \times 25 \text{ mm}^2$ with a total span of 305 mm and midspan length of 152 mm. One fourth of the beam cross-section was divided into a 10×10 grid ($n = m = 10$ in Eqs 10 and 11), in which convergence studies of MC in the middle of the cross-section and moment curvature analysis were shown to be sufficient. This discretization was used for both MC distribution calculation and beam analysis. The moment curvature relationship was evaluated at 250 equally spaced time steps of 7.2 h. Thirty divisions of the beam were used along the length, which gave four significant digits in the computed midspan deflection.

RESULTS AND DISCUSSION

Deflections of all loaded specimens measured during the bending experiment are shown in Fig 7. For both stress levels, deflection almost doubled during 75 days of loading and MC

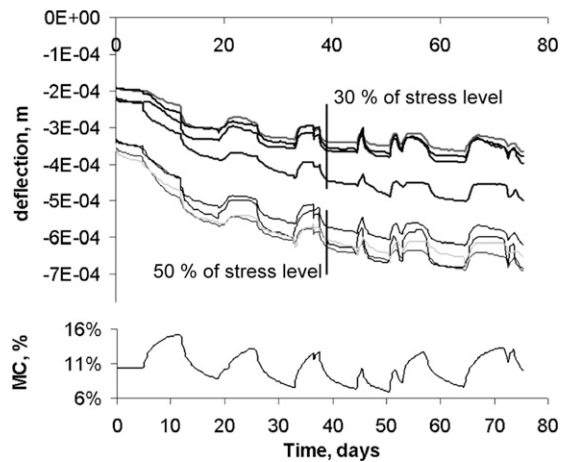


Figure 7. Measured deflection of loaded specimens at 30 and 50% of stress level and average moisture content (MC) of the reference specimen.

fluctuation. Initial MC was 10%, whereas average MC cycled between 7 and 15%.

Modeling of this behavior was based on the following assumptions and is subsequently discussed:

- linear VE behavior of wood in constant climate;
- transverse shrinkage and swelling can be expressed by shrinkage coefficient;

- mechanosorption responds differently in tension and compression zones; and
- moisture distribution and longitudinal shrinkage and swelling are symmetrically distributed across a beam cross-section.

Creep at Constant Climate and Free Hygroexpansion

Creep parameters for constant MC calculated from reference tests are shown in Table 2. Calculated creep compliance at constant climate can be seen in Fig 8. Because specimens were loaded at two stress levels, creep at constant climate was analyzed to determine whether stress level affects creep compliance. Statistical analysis was performed in two parts: analysis of creep parameters and analysis of calculated compliances at times 0, 3, and extended 10 da.

Residuals of both creep parameters and compliances were tested for normality using a Shapiro-Willkinson test. All creep parameters and

Table 2. Parameters of creep at constant climate (RH = 55%, temperature = 20°C, EMC = 10%).

Sp. no.	Stress level	Parameters		
		E_0 (Pa)	E_1 (Pa)	η (Pa.s)
1	50%	1.43×10^{10}	1.91×10^{11}	4.50×10^{16}
2		1.52×10^{10}	2.32×10^{11}	5.80×10^{16}
3		1.54×10^{10}	2.33×10^{11}	4.65×10^{16}
4		1.69×10^{10}	1.96×10^{11}	3.32×10^{16}
5	30%	1.39×10^{10}	2.34×10^{11}	4.27×10^{16}
6		1.36×10^{10}	4.04×10^{11}	9.11×10^{16}
7		1.61×10^{10}	4.43×10^{11}	6.72×10^{16}
8		1.59×10^{10}	3.69×10^{11}	7.90×10^{16}

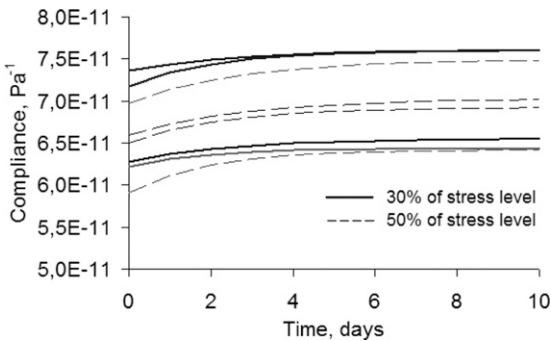


Figure 8. Fitted creep compliance at 30% (solid lines) and 50% (dashed lines) of stress level at initial constant climate extended up to 10 da of loading.

Table 3. One-way analysis of variance of fitted creep at constant climate.

	Parameters			Creep compliance at time		
	E_0	E_1	η	0 da	3 da	Extended 10 da
Distribution	Normal			Normal		
Probability ^a	0.532	0.019	0.079	0.509	0.717	0.834

^a Bold numbering stands for a nonsignificant influence. ^a Probability that the factor of stress level is not significant at alpha = 0.05.

compliances at a particular time were normally distributed (Table 3). Analysis of variance showed that the only creep parameter affected by stress level was E_1 . Total compliance was not affected by stress level, and contribution of the parameter E_1 to total compliance was small compared with material variability. Therefore, it can be concluded that stress level had no influence on creep behavior within the analyzed time range. However, the validity of this statement cannot be extended very far beyond a measured time range, but for the purposes of this hygro-mechanical modeling, creep behavior can be treated as linear with respect to stress.

Measured free shrinkage and swelling of the cross-section were compared with calculated values from measured average MC and shrinkage coefficients: 3.8% in the radial direction and 7.8% in the tangential direction (FPL 1999). As shown on the sample graph in Fig 9, measured dimensional changes in cross-section caused by MC changes matched magnitudes of predicted hygroexpansion. This is important because when modeling the hygro-mechanical response of a beam, change of cross-section caused by MC variation is a significant factor influencing reversal of deflection changes of overall beam stiffness during wetting and drying cycles.

Mechanosorptive Effect on Beam Deflection

Measured and simulated midspan deflection at a stress level of 50% of green strength is shown in Fig 10. Simulated deflection using compression and tension MS characteristics (Table 3) overestimated approximation of the experimental beam behavior. As suggested by Bengtsson (1999), MS strains inferred from the uniaxial

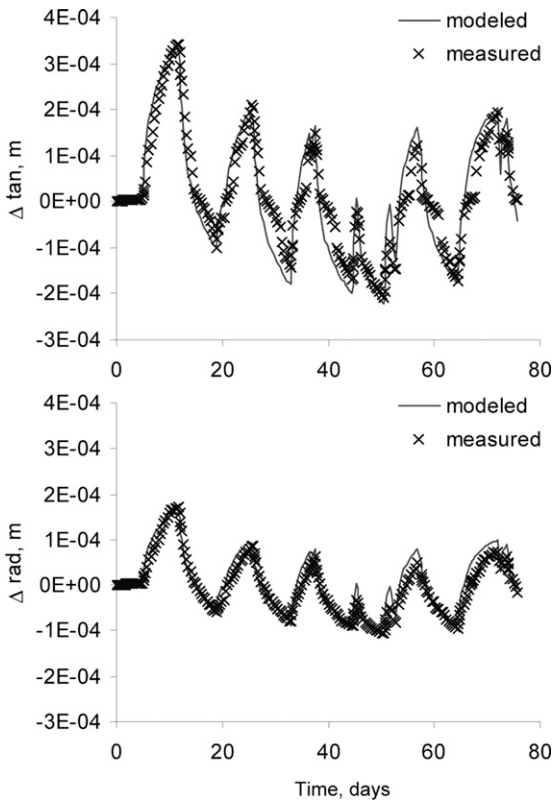


Figure 9. Measured and calculated hydroexpansion of cross-section in tangential and radial directions.

compression tests were greater than in tension tests. Gibson (1965) postulated that strain increment during MC changes could result from continuous breaking and reforming of hydrogen bonds through water movement. It appears that there is a greater potential for this breaking/reforming strain component under compression, but it is not as large as proposed by Lagaña et al (2004). When tension and compression MS element parameters are compared, the only difference that can be found is in the parameter η'_{ms2} governing long-term response. Whether the difference between MS behavior in tension and compression is significant can be resolved by performing a better designed experiment in compression or inverting the problem and adjusting the parameter η'_{ms2} to match real beam behavior. If the MS parameter in compression was set equal to the one in tension ($\eta'_{ms2} = 219.5$ GPa), the simulated deflection

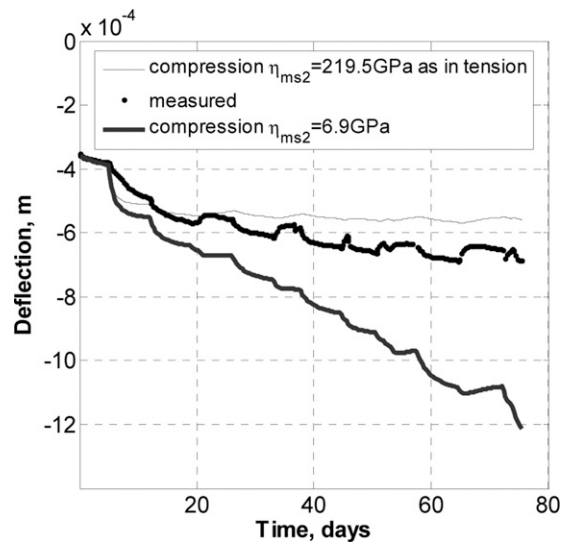


Figure 10. Comparison of simulated to measured midspan deflection at 50% of green MOR.

underestimated measured response (Fig 10). The simulated trend was better matched to midspan deflection of real beams when the parameter η'_{ms2} for compression was gradually decreased to 25 GPa (Fig 11), which was significantly different from both tension and compression parameters determined experimentally. This value was then used for all other experiments.

Simulation of total deflection and real behavior of beams loaded at two stress levels are shown in Fig 11. As expected, initial moisture change induced the most rapid change of beam stiffness. The model described typical behavior under cyclic climate conditions: deflection increased during the first moisture cycle and decreased during the next wetting cycle. This interesting effect of decreasing deflection with increasing MC has been reported in the literature (Bengtsson 1999; Houska and Koc 2000) and has been attributed to differential load-dependent longitudinal shrinkage and swelling in tension and compression (Hanhijärvi 1995).

Comments on Errors and Limitations

The model has 17 parameters (Table 1). Parameters k_{rad} , k_{tan} , and S were taken from the

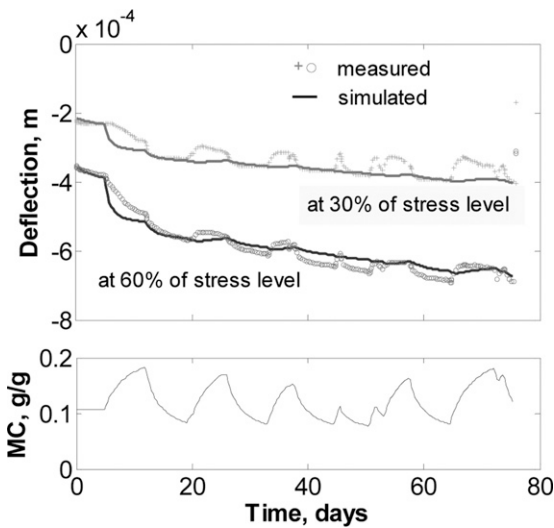


Figure 11. Comparison of simulated to measured midspan deflection at 30 and 50% of green MOR.

literature. Other parameters quantified during this study and previous studies (Lagaña 2005; Muszyński et al 2006) were measured on the representative sample size and averaged. Natural material variability can cause variability in model parameters, affecting calculated beam deflections. However, most parameters (including k_{rad} , k_{tan} , and b) are primarily responsible for changing direction of deflection, and an error in determination of these parameters results in small changes in magnitude of deflection. The overall trend in deflection is largely driven by VE and MS parameters E_1 , η , η_{ms1} , and η_{ms2} . Errors in determining these parameters have a significant effect. This was shown explicitly for η_{ms2} (Fig 10). The only way to decrease model error is to perform a large number of highly controlled material tests that are designed to isolate these parameters and take into account the effect of material variability. This was done in the case of the parameter η_{ms1} (Muszyński et al 2006). Because parameters E_1 and η were determined from initial creep of bending samples, the issue of material variation did not exist for these parameters.

Deflections simulated in this study do not account fully for deflection fluctuation caused by immediate MC changes. In this study, the phenomenon is simulated exclusively by com-

peting effects of MC-related changes in the longitudinal elastic modulus and free hygroexpansion of beam sections, which resulted in measurable changes of beam moment of inertia. No special provisions in the constitutive model were necessary. Conversely, the model is capable of predicting the overall trend in deflection, which is more important from a structural point of view.

CONCLUSIONS

An expanded comprehensive numerical approach to predict hygromechanical behavior of beams has been presented. The approach couples different MS behavior in tension and compression, time-dependent MC changes, and cross-section hygroexpansion. With material parameters from 18-h uniaxial tests, good agreement of the simulation was achieved with real behavior of a beam in cyclic climate after adjusting one MS parameter in compression. Proving that complex beam behavior in varying environments can be predicted by means of a simple constitutive model and well-defined material characteristics generated by relatively simple uniaxial experiments is important.

Although the comprehensive approach reflected critical components of bending response and overall behavior, it did not capture the rapid, transient deflection changes observed during wetting and drying cycles with sufficient accuracy. As previously discussed, one explanation may be that the difference in tensile and compressive MS effects have not been sufficiently quantified. In addition, use of an average value for transverse shrinkage and swelling of the cross-section is an approximation. A better estimate of shrinkage and swelling effects could be achieved by estimating actual time-dependent change in shape of the cross-section caused by uneven MC changes.

ACKNOWLEDGMENTS

This research was supported by the National Research Initiative of USDA Cooperative State

Research, Education and Extension Service, grant number 2001-35103-10048, and by VEGA under contract No. 1/0565/10. The research reported here is also published in Maine Agricultural and Forest Experiment Station Publication Number 3171.

REFERENCES

- Bazant ZP (1985) Constitutive equation of wood at variable humidity and temperature. *Wood Sci Technol* 19: 159-177.
- Bengtsson C (1999) Mechano-sorptive creep in wood. Part III—Mechano-sorptive tension and compression creep of spruce wood. PhD thesis, Chalmers University of Technology, Gothenburg, Sweden.
- Bengtsson C (2001) 'Short-term' mechano-sorptive creep of well-defined spruce timber. *Holz Roh Werkst* 1/2 (59):117-128.
- Crank J (1979) *Mathematics of diffusion*. 2nd edition. Oxford University Press, New York.
- Davids WG, Dagher HJ, Breton JM (2000) Modeling creep deformations of FRP-reinforced glulam beams. *Wood Fiber Sci* 4(32):426-441.
- FPL (1999) *Wood handbook: Wood as an engineering material*. Gen Tech Rep FPL-GTR-113. USDA For Serv Forest Prod Lab, Madison, WI. 463 pp.
- Gamache C (2001) Preliminary investigation on the durability of FRP-reinforced glulam bridge girders. Graduate thesis, University of Maine, Orono, ME.
- Gibson EJ (1965) Creep of wood: Role of water and effect of a changing MC. *Nature* 498:213-215.
- Grossman P (1976) Requirements for a model that exhibits mechano-sorptive behaviour. *Wood Sci Technol* 10: 163-168.
- Hanhijärvi A (1995) Modelling of creep deformation mechanism in wood. VTT publications 231. PhD thesis, Technical Research Centre of Finland, Helsinki, Finland.
- Hanhijärvi A (2000) Advances in the knowledge of the influence of moisture changes on the long-term mechanical performance of timber structures. *Mater Struct* 33 (225):43-49.
- Hanhijärvi A, Hunt DG (1998) Experimental indication of interaction between viscoelastic and mechano-sorptive creep. *Wood Sci Technol* 32:57-70.
- Houska M, Koc P (2000) Sorptive stress estimation: An important key to the mechano-sorptive effect in wood. *Mech Time-Depend Mater* 4:81-98.
- Hunt DG (1994) Present knowledge of mechanosorptive creep of wood. Pages 73-97 in *Creep in timber structures*. Report of RILEM Technical Committee 112-TSC. London, UK.
- Kretschmann DE, Green DW (1996) Modeling MC-mechanical property relationships for clear southern pine. *Wood Fiber Sci* 28:320-337.
- Lagaña R (2005) Development of small scale experimental protocol and a multi-physical model to predict the complex hygro-mechanical behavior of wood under varying climates. PhD thesis, University of Maine, Orono, ME.
- Lagaña R, Muszyński L, Shaler SM (2004) Mechano-sorptive properties of red spruce (*Picea Rubens*, Sarg.) in compression parallel to grain. Pages 143-149 in S. Kurjatko and J. Kudela, eds. *Interaction of wood with various forms of energy*. Technical University in Zvolen, Zvolen, Slovakia.
- Leicester RH (1971) A rheological model for mechano-sorptive deflections of beams. *Wood Sci Technol* 5(3):211-220.
- Lu JP, Leicester RH (1997) Mechano-sorptive effects on timber creep. *Wood Sci Technol* 31:331-337.
- Mårtensson A (1994) Creep behavior of structural timber under varying humidity conditions. *J Struct Eng* 120:437-449.
- Moutee M, Fortin Y (2007) A global rheological model of wood cantilever as applied to wood drying. *Wood Sci Technol* 41:209-234.
- Muszyński L (1997) Modeling of the drying stresses in wood. PhD thesis, Agricultural University of Poznan, Poznan, Poland [in Polish with summary in English].
- Muszyński L, Lagaña R, Shaler SM (2006) Hygro-mechanical behavior of red spruce in tension parallel to the grain. *Wood Fiber Sci* 38:155-165.
- Muszyński L, Lagaña R, Shaler SM, Davids W (2005) Comments on the experimental methodology for determination of the hygro-mechanical properties of wood. *Holzforschung* 59:232-239.
- Muszyński L, Olejniczak P (1996) A simple experimental method to determine some basic parameters for mechano-sorptive creep model for wood. Pages 479-483 in *Quality of wood drying through process modelling and novel technologies*. 5th International IUFRO Wood Drying Conference. 3.-17. August, Quebec City, Canada.
- Navi P, Pittet V, Plummer CJG (2002) Transient moisture effect on wood creep. *Wood Sci Technol* 36:447-462.
- Omarsson S (1999) Numerical analysis of moisture related distortions in sawn timber. Chapter 4. PhD thesis, Chalmers University of Technology, Sweden.
- Omarsson S, Dahlblom O, Petersson H (1998) A numerical study of the shape stability of sawn timber to moisture variation. Part 1. Theory. *Wood Sci Technol* 32:325-334.
- Perkintny T (1951) *Research on swelling pressure of wood*. Państwowe Wydawnictwo Rolnicze i Lesne, Warszawa [in Polish].
- Plevris N, Triantafillou TC (1995) Creep behavior of FRP-reinforced wood members. *J Struct Eng* 2(121):174-186.
- Ranta-Maunus A (1994) Creep analysis of timber structures. Pages 128-135 in *Creep in timber structures*. Report of RILEM Technical Committee 112-TSC. London, UK.
- Ranta-Maunus A, Gowda S (1994) Curved and cambered glulam beams. Part 2: Long-term load tests under

- cyclically varying humidity. VTT Publications 171, Espoo, Finland. 36 pp.
- Rybarczyk W (1973) A study on development of a mathematical model for the mechano-sorptive properties of certain wood-based materials. *Prace Instytutu Technologii Drewna*. 66:17-138 [in Polish with summary in English].
- Salin JG (1992) Numerical prediction of checking during timber drying and a new mechano-sorptive model. *Holz Roh Werkst* 50:195-200.
- Stamm AJ (1959) Bound water diffusion in the fiber direction. *Forest Prod J* 9:27-32.
- Strömbro J, Gudmundson P (2008) An anisotropic fibre-network model for mechano-sorptive creep in paper. *Int J Solids Struct* 45:5765-5787.
- Toratti T (1992) Creep of timber beams in a variable environment. PhD thesis, Report 31, Helsinki University of Technology, Helsinki, Finland.
- Toratti T, Svensson S (2000) Mechano-sorptive experiments perpendicular to grain under tensile and compressive loads. *Wood Sci Technol* 34:317-326.
- Wang JG (1991) A review transient moisture effects in materials. *J Mater Sci* 26:5113-5126.
- Yahiaoui K (1991) A rheological model to account for mechano-sorptive behavior. Pages 27-35 in A. Mårtensson, A. Ranta-Maunus, and I. Seoane, eds. Presentations at the COST 508 wood mechanics workshop on fundamental aspects of creep in wood, March 20-21, Lund, Sweden (Commission of the European Communities).